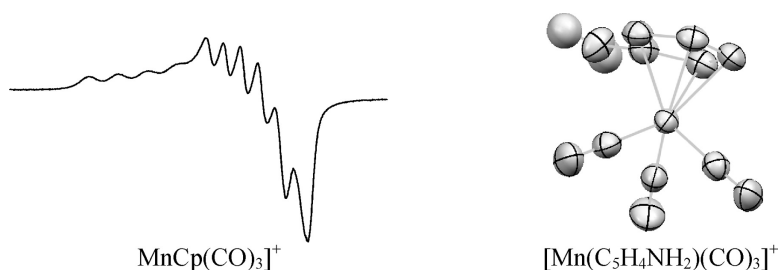Article

# Cymantrene Radical Cation Family: Spectral and Structural Characterization of the Half-Sandwich Analogues of Ferrocenium Ion

Derek R. Laws, Daesung Chong, Karen Nash, Arnold L. Rheingold, and William E. Geiger

$MnCp(CO)_3]^+$

$[Mn(C_5H_4NH_2)(CO)_3]^+$

## More About This Article

Additional resources and features associated with this article are available within the HTML version:

- Supporting Information
- Access to high resolution figures
- Links to articles and content related to this article
- Copyright permission to reproduce figures and/or text from this article

View the Full Text HTML

# Cymantrene Radical Cation Family: Spectral and Structural Characterization of the Half-Sandwich Analogues of Ferrocenium Ion

Derek R. Laws,[†] Daesung Chong,[†] Karen Nash,[†] Arnold L. Rheingold,[‡] and William E. Geiger*,[†]

*Department of Chemistry, University of Vermont, Burlington, Vermont 05405 and Department of Chemistry and Biochemistry, University of California at San Diego, La Jolla, California 92093*

Received March 14, 2008; E-mail: william.geiger@uvm.edu

***Abstract:*** The anodic one-electron oxidation of three members of the half-sandwich family of piano-stool compounds $MnCp^\gamma(CO)_3$, where $Cp^\gamma$ is a generic cyclopentadienyl ligand, has been studied in a $CH_2Cl_2$/$[NBu_4][TFAB]$ electrolyte (TFAB = $[B(C_6F_5)_4]^-$). The long-sought 17 $e^-$ radical cation of the parent complex $MnCp(CO)_3$ (cymantrene, **1**, $E_{1/2}$ = 0.92 V vs ferrocene) has been shown to be persistent in solutions that use weakly coordinating anions in place of more nucleophilic traditional electrolyte anions. Spectroscopically characterized for the first time, $\mathbf{1}^+$ was shown to absorb in the visible (530 nm), near-IR (2066 nm), and IR (2118, 1934 cm$^{-1}$) regions. It was ESR-active at low temperatures ($g_{||}$ = 2.213, $g_\perp$ = 2.079, $A_{||}$ (Mn) = 79.2 G, $A_\perp$ (Mn) = 50 G) and NMR active at room temperature ($\delta$ = 22.4 vs TMS). The radical cations of the Cp-functionalized analogues, $Mn(\eta^5\text{-}C_5H_4NH_2)(CO)_3$, **2**, $E_{1/2}$ = 0.62 V, and $MnCp^*(CO)_3$ ($Cp^*$= $\eta^5\text{-}C_5Me_5$, **3**), $E_{1/2}$ = 0.64 V, were generated electrochemically as well by the chemical oxidant $[ReCp(CO)_3]^+$. The structures of $\mathbf{2}^+$ and $\mathbf{3}^+$ were determined by X-ray crystallographic studies of their TFAB salts. Compared to the structures of the corresponding neutral compounds, the cations showed elongated Mn−C(O) bonds and shortened C−O bonds, displaying the effect of diminished metal-to-CO backbonding. The bond-length changes in the $Mn(CO)_3$ moiety were much larger in $\mathbf{3}^+$ (avg changes, Mn−C(O) = + 0.142 Å, C−O = −0.063 Å) than in $\mathbf{2}^+$ (avg changes, Mn−C(O) = + 0.006 Å, C−O = −0.003 Å). Although there were only minor changes in the metal-to-center ring distances upon oxidation of either **2** or **3**, there was decidedly less bending of the C(N) atom out of the cyclopentadienyl plane in $\mathbf{2}^+$ compared to **2**. The optical, vibrational, and magnetic resonance spectra of radicals $\mathbf{2}^+$ and $\mathbf{3}^+$ were also observed. The spectral data argue for the SOMOs of the 17-electron species being largely located on the $Mn(CO)_3$ moiety, having 40−50% Mn d-orbital character, with the ground states of the radicals, most likely $^2A''$, lying close in energy (within about 6000 cm$^{-1}$) to excited states that are responsible for their rapid electronic relaxations. The cymantrenyl moiety is proposed as an anodic redox tag (or label) having physical and chemical properties that are significantly different from those of its ferrocenyl analogue.

## Introduction

Perhaps the most highly studied half-sandwich transition metal compound is the piano-stool complex $MnCp(CO)_3$ (Cp = $\eta^5\text{-}C_5H_5$), **1**,[1,2] often referred to as cymantrene by analogy to ferrocene. One emerging area to which cymantrene is contributing is the use of organometallic tags (or labels) to alter the chemical or analytical properties of chemical targets. The most common molecular labels are those which take advantage, either directly or indirectly, of the one-electron oxidation of an attached ferrocenyl group.[3] The chief attraction in using a cymantrenyl moiety, $Mn(\eta^5\text{-}C_5H_4)(CO)_3$, in place of ferrocenyl is its electron-withdrawing and IR-active carbonyl groups.[4] Its redox chemistry, however, has been underutilized. Although the

cathodic response of cymantrenyl-labeled bovine serum albumin has been employed for immunoassays,[5] applications of cymantrenyl anodic chemistry are lacking despite the fact that the $[MnCp(CO)_3]^{0/+}$ couple has been shown to be at least partially reversible by cyclic voltammetry (CV), as will be discussed

---

† University of Vermont.
‡ University of California at San Diego.
(1) (a) Treichel, P. M. In *Comprehensive Organometallic Chemistry*; Wilkinson, G., Stone, F. G. A., Abel, E. W., Eds.; Pergamon Press: Oxford, 1982; Vol. 4, pp 123−132. (b) (Original preparation) Piper, T. S.; Cotton, F. A.; Wilkinson, G. *J. Inorg. Nucl. Chem.* **1955**, *1*, 165.

(2) For example, the following references involve applications of cymantrene in the chemistry of fuels: (a) Marsh, N. D.; Preciado, I.; Eddings, E. G.; Sarofim, A. F.; Palotas, A. B.; Robertson, J. D. *Combust. Sci. Technol.* **2007**, *179*, 987. (b) Geivanidis, S.; Pistikopoulos, P.; Samaras, Z. *Sci. Total Environ.* **2003**, *305*, 129. (c) Oxley, J. C.; Smith, J. L.; Rogers, E.; Ye, W.; Aradi, A. A.; Henly, T. J. *Energy and Fuels* **2000**, *14*, 1252Sensors: (d) Nefedov, V. A.; Polyakova, M. V.; Rorer, J.; Sabelnikov, A. G.; Kochetkov, K. A. *Mendeleev Commun.* **2007**, *17*, 167. (e) Markwell, R. D.; Butler, I. S.; Gao, J. P.; Shaver, A. *Appl. Organomet. Chem.* **1992**, *6*, 693. Chiral synthesis: (f) Ferber, B.; Top, S.; Jaouen, G. *J. Organomet. Chem.* **2004**, *689*, 4872. (g) Lyubimov, S. E.; Davankov, V. A.; Loim, N. M.; Popova, L. N.; Petrovskii, P. V.; Valetskii, P. M.; Gavrilov, K. N. *J. Organomet. Chem.* **2006**, *691*, 5980. Medicine: (h) Malisza, K. L.; Top, S.; Kaissermann, J.; Caro, B.; Senechal-Tocquer, M.; Senechal, D.; Saillard, J.; Triki, S.; Kahlal, S.; Britten, J. F.; McGlinchey, M. J.; Jaouen, G. *Organometallics* **1995**, *14*, 5273. (i) Lavastre, I.; Besancon, J.; Brossier, P.; Moise, C. *Appl. Organomet. Chem.* **1990**, *4*, 9.

below. The reasons for this underdevelopment would seem to be the relatively positive potential of the couple (*ca.* 0.9 V vs ferrocene) and the instability of the radical cation on the longer-term (spectroscopic or electrosynthetic) time scale. This paper addresses the second of these points, which we consider to be the more serious impediment to development of cymantrenyl redox tags.

The expectation that cymantrene would be significantly harder to oxidize than ferrocene owing to the presence of its strongly π-accepting carbonyl groups has been confirmed both by photoelectron spectroscopy (PES)[6,7] and by a number of electrochemical studies.[8-15] More poorly understood, however, is the dramatically reduced lifetime of the cymantrene radical cation, $1^+$, compared to the ferrocenium ion. The frontier orbitals of cymantrene and ferrocene are similar in makeup, both compounds being viewed as pseudo-octahedral systems in which the three *fac* carbonyls are topologically equivalent to the Cp anion,[16,17] with the three highest-energy filled orbitals for the $d^6$ complexes being closely spaced in energy. In the case of cymantrene, these orbitals are derived primarily from e- and a-type contributions of the Mn(CO)$_3$ moiety,[18-20] and their close

spacing has been confirmed experimentally by the finding that the lowest energy ionizations of cymantrene are unresolved by PES.[6,7] A number of groups have shown[8-12] that the one-electron anodic oxidation of **1** is at least partially chemically reversible on the CV time scale[21] in nonaqueous media, but based on the published work, even *in situ* spectral characterization of $1^+$ has apparently eluded investigators[22] (carbonyl-substituted derivatives have proven more stable, as will be discussed below). Qualitatively, it might be expected that removal of an electron from **1** would weaken the Mn—C(O) bonds (owing to reduced metal-to-CO back-bonding) and perhaps the Mn—Cp bond (depending on the nature of the SOMO of $1^+$). However, neither of these possibilities seemed, to us at least, sufficient to make the cymantrene radical cation inherently unstable under the conditions employed for its electrochemical generation. The treatment by Field et al.[7] of the highest filled orbitals of **1**, concluding that the trio of e- and a-type orbitals have significant metal—ligand mixing, further begs the question of why $1^+$ does not exhibit greater stability. We set out to see if its reported decomposition arose from follow-up reactions with the electrochemical supporting electrolyte anions, usually either [PF$_6$]$^-$ or [BF$_4$]$^-$, which are known to have modest nucleophilicity toward organometallic radical cations.[23-25] This is, indeed, the case. In this paper we show that when the cymantrene radical cation is generated in a medium consisting of CH$_2$Cl$_2$ and [NBu$_4$][B(C$_6$F$_5$)$_4$], it is persistent on a synthetic (electrolysis) time scale, allowing its broad spectral characterization (UV−vis, IR, near IR, ESR, and $^1$H NMR). Furthermore, two of its Cp-substituted analogues, namely the amino-substituted complex Mn(C$_5$H$_4$NH$_2$)(CO)$_3$, **2**,

(3) Leading references to the literature of ferrocenyl redox tags are: (a) Cuffe, L.; Hudson, R. D. A.; Gallagher, J. F.; Jennings, S.; McAdam, C. J.; Connelly, R. B. T.; Manning, A. R.; Robinson, B. H.; Simpson, J. *Organometallics* **2005**, *24*, 2051. (b) Warren, S.; McCormac, T.; Dempsey, E. *Bioelectrochemistry* **2005**, *67*, 23. (c) Ryabov, A. D. *Adv. Inorg. Chem.* **2004**, *55*, 201. (d) Beer, P. D.; Hayes, E. J. *Coord. Chem.* **2003**, *240*, 167. (e) Chaubey, A.; Malhotra, B. D. *Biosens. Bioelectron.* **2002**, *17*, 441. (f) Suzawa, T.; Ikariyama, Y.; Aizawa, M. *Anal. Chem.* **1994**, *66*, 3889. (g) Hill, H. A. O.; Sanghera, G. S. In *Biosensor: A Practical Approach*; Cass, A. E. G., Ed.; Oxford University Press: London, 1990; pp 19−46. (h) Foulds, N. C.;; Lowe, C. R. *Anal. Chem.* **1988**, *60*, 2473. (i) Cass, A. E. G.; Davis, G.; Francis, G. D.; Hill, H. A. O.; Aston, W. J.; Higgins, I. J.; Plotkin, E. V.; Scott, L. D. L.; Turner, A. P. F. *Anal. Chem.* **1984**, *56*, 667.

(4) (a) Lepore, S. D.; Khoram, A.; Bromfield, D. C.; Cohn, P.; Jairaj, V.; Silvestri, M. A. *J. Org. Chem.* **2005**, *70*, 7443–7446. (b) Zhang, Z.; Lepore, S. D. *Tetrahedron Lett.* **2002**, *43*, 7357–7360. (c) Gradén, H.; Kann, N. *Curr. Org. Chem* **2005**, *9*, 733. (d) Dorozhkin, L. M.; Nefedov, V. A.; Sabelnikov, A. G.; Sevastjanov, V. G. *Sens. Actuators, B* **2004**, *B99*, 568. (e) Salmain, M.; Vessieres, A.; Top, S.; Jaouen, G.; Butler, I. S. *J. Raman Spectrosc.* **1995**, *26*, 31. (f) Wang, Z.; Roe, B. A.; Nicholas, K. M.; White, R. L. *J. Am. Chem. Soc.* **1993**, *115*, 4399. (g) Salmain, M.; Vessieres, A.; Jaouen, G.; Butler, I. S. *Anal. Chem.* **1991**, *63*, 2323. (h) Avastre, I.; Besancon, J.; Brossier, P.; Moise, C. *Appl. Organomet. Chem.* **1990**, *4*, 9. (i) Hublau, P.; Sergheraert, C.; Ballester, L.; Dautrevaux, M. *Eur. J. Med. Chem.* **1983**, *18*, 131.

(5) (a) Hromadova, M.; Salmain, M.; Fischer-Durand, N.; Pospisil, L.; Jaouen, G. *Langmuir* **2006**, *22*, 506. (b) Hromadova, M.; Salmain, M.; Sokolova, R.; Pospisil, L.; Jaouen, G. *J. Organomet. Chem.* **2003**, *668*, 17.

(6) (a) Calabro, D. C.; Lichtenberger, D. L. *J. Am. Chem. Soc.* **1981**, *103*, 6846. (b) Lichtenberger, D. L.; Fenske, R. F. *J. Am. Chem. Soc.* **1976**, *98*, 50. These results and otherwise unpublished data have been discussed by: (c) van Dam, H.; Oskam, A. In *Transition Metal Chemistry*; Melson, G. A., Figgis, B. N., Eds.; Marcel Dekker, Inc.: New York, 1985; pp 174 ff.

(7) Field, C. N.; Green, J. C.; Moody, A. G. J.; Siggel, M. R. F. *Chem. Phys.* **1996**, *206*, 211.

(8) Huang, Y.; Carpenter, G. B.; Sweigart, D. A.; Chung, Y. K.; Lee, B. Y. *Organometallics* **1995**, *14*, 1423.

(9) Atwood, C. G.; Geiger, W. E.; Bitterwolf, T. E. *J. Electroanal. Chem.* **1995**, *397*, 279.

(10) Hershberger, J. W.; Amatore, C.; Kochi, J. K. *J. Organomet. Chem.* **1983**, *250*, 345.

(11) Kochi, J. K. *J. Organomet. Chem.* **1986**, *300*, 139.

(12) Pickett, C. J.; Pletcher, D. *J. Chem. Soc., Dalton Trans.* **1976**, 636.

(13) Denisovich, L. I.; Zakurin, N. V.; Gubin, S. P.; Ginzburg, A. G. *J. Organomet. Chem.* **1975**, *101*, C43.

(14) Plenio, H.; Burth, D. *Organometallics* **1996**, *15*, 1151. describes the poorly reversible oxidation of an indenyl Mn(CO)$_3$ complex.

(15) Munoz, R. A. A.; Banks, C. E.; Davies, T. L.; Angnes, L.; Compton, R. G. *Electroanalysis* **2006**, *18*, 621.

(16) Albright, T. A.; Burdett, J. K.; Whangbo, M-H. *Orbital Interactions in Chemistry*; John Wiley & Sons: New York, 1985; p 388

(17) Adding to the pseudo-octahedral model is the fact that the lowest unfilled orbitals in cymantrene and ferrocene are nearly degenerate sets of e$_1''$-type cyclopentadienyl π-orbitals that are metal-antibonding.

(18) Mingos, D. M. P. In *Comprehensive Organometallic Chemistry*; Wilkinson, G., Stone, F. G. A., Abel, E. W., Eds.; Pergamon Press: Oxford, 1982; Vol. 3, pp 28−46.

(19) (a) Schilling, B. E. R.; Hoffmann, R.; Lichtenberger, D. L. *J. Am. Chem. Soc.* **1979**, *101*, 585. (b) Elian, M.; Chen, M. M. L.; Mingos, D. M. P.; Hoffmann, R. *Inorg. Chem.* **1976**, *15*, 1148.

(20) Reference 16, p 385.

(21) Under normal experimental conditions, the maximum CV time scale is approximately 10 s.

(22) The ESR spectrum assigned to $1^+$ from a solution of bulk-electrolyzed cymantrene (ref 12) almost certainly arose from a decomposition product. As shown in the present work, the cymantrene radical cation is ESR-silent under the fluid room-temperature conditions employed in that work and the spectral characteristics ($\langle g \rangle$ = 2.015, $\langle A \rangle_{Mn}$ = 92.5 G) are typically found in Mn(II) solvento complexes. A similar spectrum assigned to a cymantrenyl-based radical cation observed after iodine oxidation of Mn($\eta^5$-C$_5$H$_4$Me)(CO)$_2$(C(O)-ferrocenyl) (see ref 33) ($\langle g \rangle$ = 2.037, $\langle A \rangle_{Mn}$ = 91.6 G) is also likely to have arisen from radical decomposition.

(23) Stone, N. J.; Sweigart, D. A.; Bond, A. M. *Organometallics* **1986**, *5*, 2553.

(24) Hill, M. G.; Lamanna, W. M.; Mann, K. R. *Inorg. Chem.* **1991**, *30*, 4687.

(25) Camire, N.; Nafady, A.; Geiger, W. E. *J. Am. Chem. Soc.* **2002**, *124*, 7260.

(26) (a) Bernal, I.; Korp, J. D.; Herrmann, W. A.; Serrano, R. *Chem. Ber.* **1984**, *117*, 434. (b) Hughes, R. P.; Hemond, R. C.; Locker, H. B. *Organometallics* **1986**, *5*, 2391.

(27) (a) Chong, D.; Nafady, A.; Costa, P. J.; Calhorda, M. J.; Geiger, W. E. *J. Am. Chem. Soc.* **2005**, *127*, 15676. (b) Chong, D.; Laws, D. R.; Nafady, A.; Costa, P. J.; Rheingold, A. L.; Calhorda, M. J.; Geiger, W. E. *J. Am. Chem. Soc.* **2008**, *130*, 2692.

(28) (a) Regitz, M.; Hocker, J.; Liedhegener, A. *Org. Synth.* **1973**, *5*, 179. (b) Manuel, T. A. *Adv. Organomet. Chem.* **1965**, *3*, 181. (see especially p 221)

(29) LeSuer, R. J.; Buttolph, C.; Geiger, W. E. *Anal. Chem.* **2004**, *76*, 6395.

***Table 1.*** Infrared Spectroscopy Data for Compounds Dissolved in CH$_2$Cl$_2$ at 298 K$^{a,b}$

| | $E_{1/2}$ (V) | $\nu_{sym}$ (cm$^{-1}$) | $\nu_{asym}$ (cm$^{-1}$) | $\nu_{CO}$ (cm$^{-1}$) |
|---|---|---|---|---|
| **1** | 0.92 | 2022 (2020) | 1934 (1932) | 1963 |
| **1$^+$** | | 2118 (2116) | 2058 (2061, 2050) | 2078 |
| **2** | 0.62 | 2012 | 1921 | 1951 |
| **2$^+$** | | 2084 | 2032 | 2049 |
| **3** | 0.64 | 2004 | 1917 | 1946 |
| **3$^+$** | | 2093 | 2033 | 2053 |

$^a$ $\nu_{CO} = (\nu_{sym} + 2\nu_{asym})/3$. $^b$ Values in parentheses are data at 253 K.

and MnCp*(CO)$_3$ (Cp* = $\eta^5$-C$_5$Me$_5$), **3**, were similarly characterized by electrochemistry and spectroscopy. In the cases of the latter two complexes, their 17-electron cations were isolated as TFAB salts (TFAB = [B(C$_6$F$_5$)$_4$]$^-$) and structurally characterized by single crystal X-ray analysis. The picture that emerges is that the cymantrenyl group, Mn($\eta^5$-C$_5$H$_4$)(CO)$_3$, holds promise as an anodic spectroelectrochemical molecular label that can be considered as an alternative to its widely employed ferrocenyl predecessor.



R = H (**1**),
= NH$_2$ (**2**)

**3**
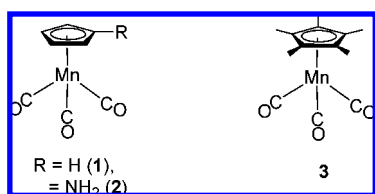
## Experimental Section

**Materials.** Schlenk-type procedures under nitrogen were used for all synthetic procedures. MnCp(CO)$_3$ was supplied by Strem Chemical Co. and used as received. MnCp*(CO)$_3$[26] and [(ReCp(CO)$_3$)$_2$][B(C$_6$F$_5$)$_4$]$_2$[27] were prepared as described in the literature. CDCl$_3$ and CD$_2$Cl$_2$ were purchased from Cambridge Isotope Laboratories, Inc. and used as received for NMR experiments. *n*-BuLi, 1.6 M in hexanes, was used as supplied by Acros. Tosyl azide was prepared according to a literature procedure.[28a] [NBu$_4$][B(C$_6$F$_5$)$_4$] was prepared by metathesis[29] of [NBu$_4$]Br with K[B(C$_6$F$_5$)$_4$] (Boulder Scientific Co.) in MeOH, recrystallized three times from CH$_2$Cl$_2$/OEt$_2$, and dried at 80 °C under vacuum for 24 h. [NBu$_4$][PF$_6$] was supplied by Acros, recrystallized from EtOH three times, and dried at 80 °C under vacuum for 24 h. Compounds of the type MnCp(CO)$_2$L (L = PPh$_3$, PCy$_3$ (Cy = cyclohexyl), P(*p*-MeOPh)$_3$, P(*p*-MePh)$_3$, P(*p*-FPh)$_3$, P(*p*-CF$_3$Ph)$_3$) were prepared using photolysis procedures.[28b] CH$_2$Cl$_2$ was dried over calcium hydride and collected by vacuum transfer prior to use. CDCl$_3$ used for controlled potential electrolysis was dried over 4 Å molecular sieves for 5 days and collected by vacuum transfer prior to use. THF was dried over potassium and collected by vacuum transfer from potassium benzophenone.

**Mn(C$_5$H$_4$NH$_2$)(CO)$_3$, 2.** This compound was prepared through an adaptation of a literature procedure.[30] 2.00 g (9.8 mmol) of **1** were reacted with 6.25 mL (10.0 mmol) of *n*-BuLi (1.6 M in hexanes) in THF at −78 °C. After stirring for 1 h, 2.19 g (11.1 mmol) of tosyl azide were added, and the mixture was allowed to warm to room temperature. After 14 h, the solvent was removed *in vacuo* and the remaining black residue was dissolved in 35 mL of 95% EtOH. 2.10 g (10.7 mmol) of Na[BH$_4$] dissolved in 35 mL of 95% EtOH were added, and an exothermic reaction was observed. It was allowed to proceed for 45 min, followed by solvent removal *in vacuo*. The oily solid was extracted with 5 × 20 mL of OEt$_2$, after which the solvent was evaporated, yielding a dark orange oil. Warm (50 °C) hexanes, 5 × 30 mL, were then used to extract

a mixture of **2** and any remaining **1**. The resulting yellow solution was slowly evaporated under a stream of nitrogen until yellow crystals began to form. The mixture was then cooled at −20 °C for 1 h, yielding 0.86 g (3.92 mmol, 40%) of pure **2** as yellow crystals. X-ray quality crystals were obtained by dissolving 20 mg of **2** in 2 mL of warm hexanes and allowing the solution to sit at room temperature for 2 days. Anal. Calcd for **2**: C, 43.87; H, 2.74; N, 6.40. Found: C, 44.03; H, 2.83; N, 6.38. IR (CH$_2$Cl$_2$): $\nu_{NH}$ 3458 w, 3386 w, $\nu_{CO}$ 2012 s, 1921 vs, cm$^{-1}$. $^1$H NMR (CDCl$_3$): $\delta$ (ppm) 4.52 (t), 2H, 4.26 (t), 2H.

**Instrumentation.** $^1$H NMR spectra were acquired on a Bruker ARX 500 MHz spectrometer, and ESR spectra were recorded using a Bruker ESP 300E spectrometer. Infrared data were acquired on an ATI-Mattson infinity series FT-IR interfaced to a computer employing Winfirst software at a resolution of 4 cm$^{-1}$. For spectroelectrochemistry, a mid-IR fiber-optic "dip" probe (Remspec, Inc.) was used in conjunction with the Mattson FT-IR, as described earlier.[31] UV−vis and near-IR spectroscopic data were collected on a Cary Olis-14 spectrometer using a quartz cuvette with a path length of 1 cm.

**Electrochemistry.** All electrochemistry except IR spectroelectrochemistry was conducted in a Vacuum Atmospheres drybox under nitrogen, using a Princeton Applied Research (PAR) Model 273A potentiostat interfaced to a personal computer. Working electrodes were glassy carbon electrodes (GCEs) and platinum electrodes supplied by Bioanalytical Systems. The electrode surfaces were pretreated using a standard sequence of polishing with diamond paste (Buehler) of decreasing sizes (3 to 0.25 $\mu$m) interspersed by washings with nanopure water and finally vacuum drying. For controlled potential coulometry, a platinum mesh basket was used as the working electrode. The reference electrode in all cases was a Ag/AgCl wire separated from solution by a fine frit, but all potentials have been recorded versus the FeCp$_2^{0/+}$ redox couple obtained by using FeCp$_2$ as an internal standard.[32] Data used in cyclic voltammetry (CV) simulations were collected using positive-feedback *iR* compensation to minimize resistance and were background-subtracted using CV scans collected with only solvent and electrolyte present. Digital simulations were performed using Digisim 3.0 (Bioanalytical Systems).

**Preparation of [2][B(C$_6$F$_5$)$_4$] and [3][B(C$_6$F$_5$)$_4$].** Analytically pure **2$^+$** was prepared by dissolving 10 mg (4.57 × 10$^{-5}$ mol) of **2** in 1.0 mL of CH$_2$Cl$_2$ and adding 50 mg (1.99 × 10$^{-5}$ mol) of solid [(ReCp(CO)$_3$)$_2$][B(C$_6$F$_5$)$_4$]$_2$. This ratio provides about 0.8 equiv of the monomer cation [ReCp(CO)$_3$]$^+$ as the oxidizing agent. The original yellow solution turned dark green immediately. After 5 min, 4 mL of hexanes were added dropwise over the next 5 min, resulting in the precipitation of green **[2][B(C$_6$F$_5$)$_4$]**. The product was washed with copious amounts of hexanes, yielding 25 mg of product (70% based on oxidant). Alternatively, the isolation of [**2**][B(C$_6$F$_5$)$_4$] was achieved by the above method using CDCl$_3$ in place of CH$_2$Cl$_2$, a solvent in which [**2**][B(C$_6$F$_5$)$_4$] is insoluble. The product precipitated as the reaction proceeded, and after 10 min the solvent was decanted and the product washed with excess CDCl$_3$. X-ray quality crystals were prepared by dissolving 10 mg of [**2**][B(C$_6$F$_5$)$_4$] in 0.5 mL of CH$_3$NO$_2$ and adding a small amount (⟨0.5 mL) of CH$_2$Cl$_2$. The solution was stored at −20 °C for about a week, at which time crystals were collected and washed with cold CH$_2$Cl$_2$.

Analytically pure **3$^+$** was prepared by dissolving 7.8 mg (2.85 × 10$^{-5}$ mol) of **3** in 1.0 mL of CH$_2$Cl$_2$ (or CD$_2$Cl$_2$) and adding 28.5 mg (1.13 × 10$^{-5}$ mol, 0.80 equiv) of solid [(ReCp(CO)$_3$)$_2$][B(C$_6$F$_5$)$_4$]$_2$. The original yellow solution turned dark green immediately. After 5 min, 6 mL of hexanes were added dropwise over the next 5 min, resulting in the precipitation of turquoise **[3][B(C$_6$F$_5$)$_4$]**. The product was washed with excess hexanes to remove unreacted **3** as well as the reaction product

(30) Holovics, T. C.; Deplazes, S. F.; Toriyama, M.; Powell, D. R.; Lushington, G. H.; Barybin, M. V. *Organometallics* **2004**, *23*, 2927.

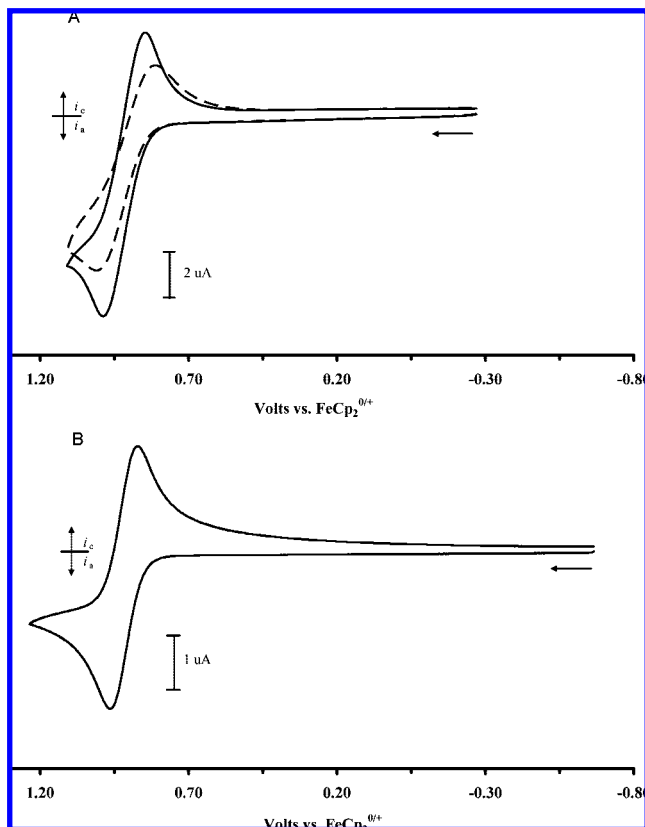(31) Shaw, M. J.; Geiger, W. E. *Organometallics* **1996**, *15*, 13.
(32) (a) Gritzner, G.; Kuta, J. *Pure Appl. Chem.* **1984**, *56*, 461. (b) Connelly, N. G.; Geiger, W. E. *Chem. Rev.* **1996**, *96*, 877.

**Figure 1.** (A) 1.0 mM **1** in $CH_2Cl_2$/0.1 M [$NBu_4$][$PF_6$] at 298 K. 1 mm GCE, 0.1 V s$^{-1}$. Solid line: first scan. Dashed line: 10th consecutive scan. (B) 0.6 mM **1** in $CH_2Cl_2$/0.05 M [$NBu_4$][$B(C_6F_5)_4$] at 298 K, 1 mm GCE, 0.1 V s$^{-1}$.

ReCp(CO)$_3$, yielding 14 mg of product (65% based on oxidant). X-ray quality crystals were obtained by dissolving 10 mg of [**3**][$B(C_6F_5)_4$] in 0.5 mL of $CH_2Cl_2$ and layering the solution with 0.5 mL of hexanes. The mixture was cooled to −20 °C for 3 days, at which time crystals were collected and washed with hexanes.

**$^1$H NMR Spectroscopy.** The spectrum of **1**$^+$ was obtained by performing controlled potential electrolysis of 3.0 mM **1** in CDCl$_3$/0.05 M [$NBu_4$][$B(C_6F_5)_4$] and preparing the NMR sample under nitrogen in the drybox. The spectra of **2**$^+$ and **3**$^+$ were obtained by addition of the appropriate amount of the chemical oxidant [(ReCp(CO)$_3$)$_2$][$B(C_6F_5)_4$]$_2$ to a 3.0 mM solution of **2** or **3** in CD$_2$Cl$_2$ in the drybox. To obtain samples with both **3** and **3**$^+$ present in varying concentrations, the solid chemical oxidant was added to the NMR sample in sequential steps, with spectra collected between additions.

**X-ray Crystallography.** Data were collected on a Bruker D8 platform diffractometer equipped with an APEX CCD detector. The structures were solved by Patterson projections. All non-hydrogen atoms were refined anisotropically, and the hydrogen atoms were placed in idealized locations. All software was contained in the SMART, SAINT, and SHELXTL libraries distributed by Bruker AXS, Madison, WI.

## Results and Discussion

**Anodic Electrochemistry.** In terms of the literature background for this study, the anodic electrochemistry of cymantrene and its methylcyclopentadienyl analogue Mn($\eta^5$-C$_5$H$_4$Me)(CO)$_3$ have been the subject of a number of papers which are in agreement that the oxidation is a one-electron process.[8–15,23] Depending on the medium, the radical cations may be sufficiently stable on a CV time scale that the 0/+ couple is at least partially chemically reversible, especially at reduced
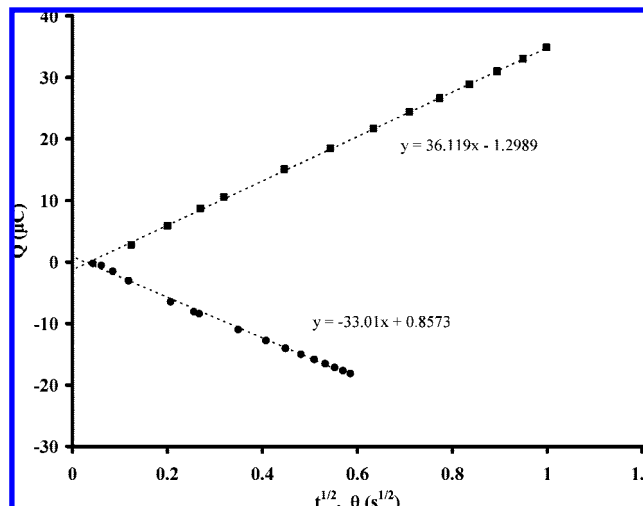


**Figure 2.** Anson plot for oxidation wave of 1.1 mM **1** in $CH_2Cl_2$/0.1 M [$NBu_4$][$PF_6$] at 298 K. Step time 1 s, 3 mm GCE.

temperatures, a fact that allowed for the study of carbonyl substitution reactions by cyclic voltammetry.[8] Spectral characterization of the radical cations was blocked, however, either by electrode passivation effects[9] or by decomposition on an electrolysis time scale.[12,22] Optical and ESR studies of this family of radicals has required substitution of one or more of the carbonyls by donor ligands, which has the effect of greatly enhancing the lifetimes of the radical cations.[8–10,33–38]

**MnCp(CO)$_3$, 1.** Although the anodic behavior of **1** is close to chemically reversible[39] at scan rates greater than 0.1 V s$^{-1}$ in $CH_2Cl_2$ solutions containing either [$PF_6$]$^-$ or [$BF_4$]$^-$ as the electrolyte anion ($E_{1/2}$ = 0.92 V vs FeCp$_2^{0/+}$, Table 1), multiple scans gave evidence of product adsorption and partial passivation of the electrode surface (see Figure 1A). The voltammetry in $CH_2Cl_2$/[$NBu_4$][$B(C_6F_5)_4$] electrolyte (also $E_{1/2}$ = 0.92 V) did not exhibit electrode history problems, consistent with increased solubility of the radical cation as the TFAB salt (Figure 1B). Double potential step chronoamperometry conducted in $CH_2Cl_2$/0.1 M [$NBu_4$][$PF_6$] at a 3 mm GCE produced an Anson plot[40] (Figure 2) that indicated only weak adsorption of [**1**][$PF_6$], as evidenced in the similar slopes for the oxidation and reduction (ratio = 0.91) and the very small extrapolated surface charges. However, **1**$^+$ was shown to undergo slow follow-up reactions when produced in the presence of [$PF_6$]$^-$. A number of controlled potential electrolyses carried out on **1** using $E_{appl}$ = 1.3 V at 298 K in $CH_2Cl_2$/0.1 M [$NBu_4$][$PF_6$] gave coulomb counts of 3−4 F, indicating decomposition of **1**$^+$ and production of other electroactive products. The resulting black solutions only showed evidence of unknown products having irreversible cathodic waves at $E_{pc}$ = −0.48 V and −1.34 at 0.1 V/s (Figures SM1, SM2). An irreversible anodic wave was also observed at $E_{pa}$ = 1.39 V. Furthermore, IR spectros-

(33) McCleverty, J. A.; Orchard, D. G.; Connor, J. A.; Lloyd, J. P.; Rose, P. D. *J. Organometal. Chem.* **1971**, *30*, C75.
(34) Treichel, P. M.; Wagner, K. P.; Mueh, H. J. *J. Organomet. Chem.* **1975**, *86*, C13.
(35) Connelly, N. G.; Kitchen, M. D. *J. Chem. Soc., Dalton Trans.* **1977**, 931.
(36) Würminghausen, T.; Sellmann, D. *J. Organomet. Chem.* **1980**, *199*, 77.
(37) Atwood, C. G.; Geiger, W. E. *J. Am. Chem. Soc.* **2000**, *122*, 5477.
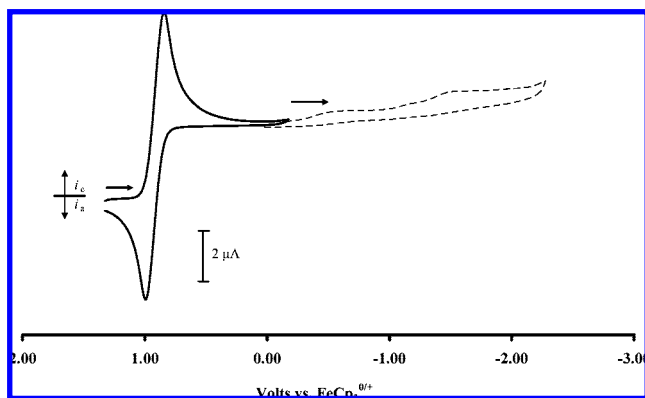(38) Pike, R. D.; Rieger, A. L.; Rieger, P. H. *J. Chem. Soc., Faraday Trans. 1* **1989**, *85*, 3913.

**Figure 3.** CVs after bulk oxidation at 1.1 V of 4.0 mM **1** in CH$_2$Cl$_2$/0.05 M [NBu$_4$][B(C$_6$F$_5$)$_4$] at 298 K. 1 mm GCE, 0.1 V s$^{-1}$. The solid line shows the scan from 1.3 V to $-$0.2 V, and the dashed line is from $-$0.2 to $-$2.4 V.



**Figure 4.** In situ IR spectroelectrochemistry of 5.0 mM **1** in CH$_2$Cl$_2$/0.05 M [NBu$_4$][B(C$_6$F$_5$)$_4$] at 253 K recorded during bulk electrolysis at $E_{app}$ = 1.1 V.

copy on the electrolyzed solution showed no evidence of metal−carbonyl species except for a small amount of unconverted **1**. The [PF$_6$]$^-$ anion is thus seen to affect **1**$^+$ in two ways: through weak adsorption as [**1**][PF$_6$] onto solid electrodes and as a nucleophile leading to decomposition of the 17 e$^-$ species. As shown below, electrochemistry in media containing weakly coordinating anion supporting electrolytes minimizes or eliminates both of these problems.

When oxidized in CH$_2$Cl$_2$/0.05 M [NBu$_4$][B(C$_6$F$_5$)$_4$] using $E_{appl}$ = 1.1 V, **1** released 0.95 F at 298 K as the solution turned a deep purple. CV scans on the electrolyzed solution showed a reversible reduction attributed to **1**$^+$ and some minor cathodic follow-up product waves at negative potentials (Figure 3). IR of the electrolysis solution showed two strong absorptions with a weighted average value of $\langle \nu_{CO} \rangle$ = 2078 cm$^{-1}$ ($\langle \nu_{CO} \rangle = (\nu_{sym} + 2\nu_{asym})/3$), a shift of 115 cm$^{-1}$ from that of neutral **1**, in the range expected for the one-electron oxidation of a "piano-stool" complex.[41] The individual carbonyl stretching frequencies for the neutral and cationic forms of **1**−**3** are collected in Table 1. Controlled potential back-electrolysis at 0.5 V regenerated **1** in 90% yield, as determined by coulometry and linear sweep voltammetry. When the bulk oxidation of **1** was carried out at 263 K, no side products were observed, and **1** was regenerated in quantitative yield. An *in situ* IR-spectroelectrochemical experiment performed on this system at 253 K gave a clean conversion to the radical cation (Figure 4), with the asymmetric pair of carbonyl bands being resolved at this temperature. Taken together, the combined electrochemical and IR data indicate that the cymantrene radical cation is highly persistent at or near room
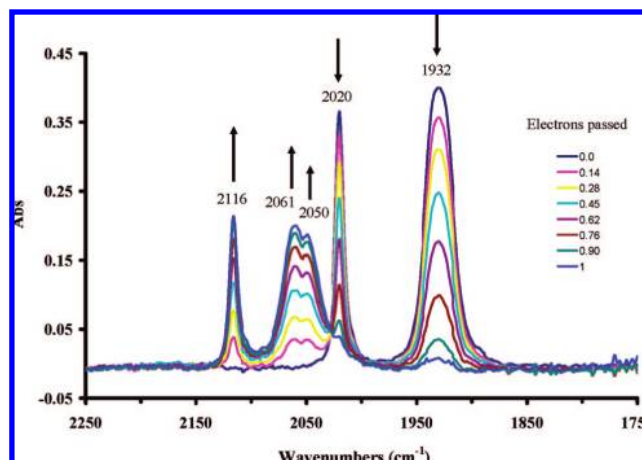
temperature in this benign electrolyte medium. Further spectral characterizations of **1**$^+$ are presented below.

**Mn(C$_5$H$_4$NH$_2$)(CO)$_3$, 2, and MnCp*(CO)$_3$, 3.** Compounds **2** and **3** exhibited anodic behavior similar to that of the parent complex **1**. The $E_{1/2}$ values shifted positive to 0.62 and 0.64 V, for **2** and **3**, respectively, in accord with the expected cyclopentadienyl substituent effects.[42] Consecutive anodic electrolysis and cathodic back electrolysis in CH$_2$Cl$_2$/[NBu$_4$][B(C$_6$F$_5$)$_4$] at 298 K regenerated about 55% of **2** and 60% of **3**, with some electroactive side products being formed (Figure SM3). The colors of the radical cations were green for **2**$^+$ and vibrant turquoise for **3**$^+$, with weighted average IR spectral shifts of 98 and 107 cm$^{-1}$ being seen for the respective radical cations (Table 1). Electrochemistry of **3** performed in CH$_2$Cl$_2$/ [NBu$_4$][PF$_6$] again gave evidence of electrode passivation and partial decomposition of **3**$^+$. In this case 2 F of charge were released, and some of the primary radical cation was present in the electrolysis solution. The major feature of the decomposition product was an anodic wave at $E_{pa}$ = 1.39 V, the same potential as seen for the decomposition product of **1**$^+$ in media containing [PF$_6$]$^-$, suggesting that the decomposition process involves cleavage of the Mn−cyclopentadienyl bond.

**Crystal Structures of [2][B(C$_6$F$_5$)$_4$] and [3][B(C$_6$F$_5$)$_4$].** TFAB salts of **2**$^+$ and **3**$^+$ were isolated through chemical oxidation of the neutral complexes by the strong one-electron oxidant [ReCp(CO)$_3$]$^+$.[27] In terms of oxidizing power, the intrinsic $E^{o'}$ of the [ReCp(CO)$_3$]$^{0/+}$ couple (1.16 V) is modified by equilibration of the monomer cation with the dimer dication [Re$_2$Cp$_2$(CO)$_6$]$^{2+}$, giving an effective $E_{1/2}$ of 1.0 V vs ferrocene in CH$_2$Cl$_2$ at room temperature.[27b] This potential provides a strong driving force for the oxidations of **2** ($E_{1/2}$ = 0.62 V) and **3** ($E_{1/2}$ = 0.64 V).

Crystalline [**2**][B(C$_6$F$_5$)$_4$] is an air-sensitive green solid, the structure of which is shown in Figure 5. Table 2 lists the collection parameters and crystal data for this sample, and Table

(39) Double potential step choronocoulometry (DPSCC), a useful technique for determination of chemical reversibility (Bard, A. J.; Faulkner, L. R. *Electrochemical Methods*; John Wiley & Sons: New York, 2001; pp 201−210) was carried out on a solution of **1** in this medium, and values for $i_{rev}/i_{fwd}$ at $2\tau$ are less than 0.20 for all step times (from 0.5 to 5 s). A model system such as ferrocene in the same medium gave values of 0.26−0.28 for the same step times, showing that **1**$^+$ is not quantitatively reduced back to **1** due to its decomposition.

(40) (a) Anson, F. C. *Anal. Chem.* **1966**, *38*, 54. (b) Anson, F. C.; Osteryoung, R. *J. Chem. Educ.* **1983**, *60*, 293.

(41) (a) Brownie, J. H.; Baird, M. C.; Laws, D. R.; Geiger, W. E. *Organometallics* **2007**, *26*, 5890. (b) Ehlers, A. W.; Ruiz-Morales, Y.; Baerends, E. J.; Ziegler, T. *Inorg. Chem.* **1997**, *36*, 5031. (c) Willner, H.; Aubke, F. *Angew. Chem., Int. Ed.* **1997**, *36*, 2402. (d) Goldman, A. S.; Kogh-Jespersen, K. *J. Am. Chem. Soc.* **1996**, *118*, 12159. (e) Nakamoto, K. *Infrared and Raman Spectra of Inorganic and Coordination Compounds*, 4th ed.; Wiley: New York, 1986; pp 292−293.

(42) Lu, S.; Stelets, V. V.; Ryan, M. F.; Pietro, W. J.; Lever, A. B. P. *Inorg. Chem.* **1996**, *35*, 1013.

(43) Sunkel, K.; Birk, U.; Soheili, S.; Stramm, C.; Teuber, R. *J. Organomet. Chem.* **2000**, *599*, 247.

(44) (a) Perrine, C. L.; Zeller, M.; Woolcock, J.; Hunter, A. D. *J. Chem. Crystallogr.* **2005**, *35*, 717. (b) Shafir, A.; Power, M. P.; Whitener, G. D.; Arnold, J. *Organometallics* **2000**, *19*, 3978. (c) Inyushin, S.; Shafir, A.; Sheats, J. E.; Minihane, M.; Witten, C. E.; Arnold, J. *Polyhedron* **2004**, *23*, 2937.
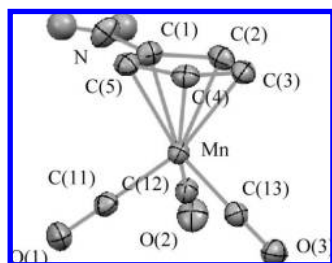
**Figure 5.** Diagram of the molecular structure of [**2**][B(C₆F₅)₄] with 50% probability ellipsoids. Cp hydrogens and counteranion omitted for clarity.

**Table 2.** X-ray Data Collection Parameters

|  | MnC₈H₆NO₃, **2** | MnC₃₂H₁₄BF₂₀NO₇, **2**⁺ | MnC₃₇H₁₅BF₂₀O₃, **3**⁺ |
|---|---|---|---|
| molecular weight | 219.08 | 970.19 | 953.24 |
| space group | $P_{bca}$ | $P\bar{1}$ | $P_{ca}2(1)$ |
| $a$ (Å) | 7.242(2) | 11.1365(8) | 16.467(2) |
| $b$ (Å) | 13.408(4) | 11.5717(8) | 11.6868(17) |
| $c$ (Å) | 17.835(5) | 14.7086(10) | 18.850(3) |
| α (deg) | 90 | 101.3260(10) | 90 |
| β (deg) | 90 | 111.6160(10) | 90 |
| γ (deg) | 90 | 102.7390(10) | 90 |
| $D_{(calc)}$ (g/cm⁻³) | 1.681 | 1.969 | 1.745 |
| volume (Å³) | 1731.8(8) | 1636.3(2) | 3627.5(9) |
| λ (Å) | 1.493 | 0.572 | 0.506 |
| Z | 8 | 2 | 4 |
| temp (K) | 208(2) | 100(2) | 208(2) |
| μ(Mo Kα) (cm⁻¹) | 0.711 | 0.711 | 0.711 |
| θ range | 2.28°–28.35° | 1.56°–28.22° | 1.74°–25.99° |
| data collected (h, k, l) | −8 ≤ h ≤ 9 | − 9 ≤ h ≤ 14 | −19 ≤ h ≤ 20 |
|  | −17 ≤ k ≤ 16 | −15 ≤ k ≤ 15 | −14 ≤ k ≤ 14 |
|  | −22 ≤ l ≤ 23 | −19 ≤ l ≤ 12 | −22 ≤ l ≤ 10 |
| no. of reflns collected | 13 747 | 10 223 | 16 435 |
| no. of indep obsd reflns ($F_0 > 2\sigma(F_0)$) | 2026 | 6206 | 5451 |
| $R(F)$ ($I > 2\sigma(I)$) | 0.0287 | 0.0462 | 0.0429 |
| $R(wF)$ ($I > 2\sigma(I)$) | 0.0679 | 0.1099 | 0.1045 |
| GOF | 1.049 | 1.062 | 1.055 |
| largest diff peak/hole (e Å⁻³) | 0.283/−0.323 | 0.599/−0.407 | 0.499/−0.180 |

**3** lists selected bond distances and angles. The structure of neutral **2** had not been previously solved, so a structure is given in Figure 6 with collection parameters and relevant bond distances and angles supplied in Tables 2 and 3. Unlike [**3**][B(C₆F₅)₄] (*vide infra*), all three CO−Mn−CO bond angles for both **2** and **2**⁺ remain close to the octahedral value 90°. In compound **2**, the C(N) atom is bent away from the metal by 4.34° with respect to the C₄ plane occupied by the four C(H) carbons of the cyclopentadienyl ligand (the three points used for this calculation are those of the C(N) atom, the midpoint of the two carbon atoms adjacent to the C(N) atom, and the point on the C₄ plane closest to the C(N) atom). This slight bending of the Cp ring is similar to the angle 4.86° which we calculate from data reported for the position of the C(N) atom in Mn(η⁵-C₅H₃ClNH₂-1,2)(CO)₃[43] and to the average angle 4.44° calculated for four 18-electron aminocyclopentadienyl iron and cobalt complexes.[44] In the 17-electron species **2**⁺, the cyclopentadienyl

**Table 3.** Selected Bond Lengths (Å) and Bond Angles (deg) for Mn(η⁵-C₅H₄NH₂)(CO)₃, **2**, and [Mn(η⁵-C₅H₄NH₂)(CO)₃]⁺, **2**⁺

| bond or angle | Mn(η⁵-C₅H₄NH₂)(CO)₃ | [Mn(η⁵-C₅H₄NH₂)(CO)₃]⁺ |
|---|---|---|
| Mn−C(1) | 2.2318(19) | 2.127(3) |
| Mn−C(2) | 2.151(2) | 2.155(3) |
| Mn−C(3) | 2.118(2) | 2.149(3) |
| Mn−C(4) | 2.115(2) | 2.149(3) |
| Mn−C(5) | 2.155(2) | 2.152(3) |
| Mn−C(11) | 1.794(2) | 1.798(3) |
| Mn−C(12) | 1.790(2) | 1.801(3) |
| Mn−C(13) | 1.795(2) | 1.799(3) |
| O(1)−C(11) | 1.152(3) | 1.147(4) |
| O(2)−C(12) | 1.152(3) | 1.149(3) |
| O(3)−C(13) | 1.147(3) | 1.144(4) |
| C(1)−C(5) | 1.412(3) | 1.407(4) |
| C(1)−C(2) | 1.424(3) | 1.423(4) |
| C(2)−C(3) | 1.420(3) | 1.417(4) |
| C(3)−C(4) | 1.411(3) | 1.418(4) |
| C(4)−C(5) | 1.428(3) | 1.418(4) |
| N−C | 1.380(2) | 1.461(4) |
| Mn-to-center C₄ | 1.782 | 1.776 |
| C(11)−Mn−C(12) | 92.22(10) | 92.16(14) |
| C(11)−Mn−C(13) | 95.06(10) | 90.85(14) |
| C(12)−Mn−C(13) | 91.35(10) | 90.01(13) |
| O(1)−C(11)−Mn | 177.2(2) | 179.0(3) |
| O(2)−C(12)−Mn | 179.08(19) | 178.1(3) |
| O(3)−C(13)−Mn | 178.6(2) | 179.2(3) |

ring approaches planarity, with only a 1.00° bending away of the C(N) carbon. In contrast, bendings of the two cyclopentadienyl rings in [(aminocyclopentadienyl)₂Fe]⁺ are considerably larger at 6.20° and 6.40°.[44c] Concomitant with alterations of the Cp bending are changes in the metal−C(N) bond lengths. Thus, the Mn−C(N) distance decreases by 0.113 Å in going from **2** to **2**⁺, whereas the Fe−C(N) distance increases by 0.105 Å in going from the ferrocene to ferrocenium-type systems in [(aminocyclopentadienyl)₂Fe]⁰/⁺. Changes in the C−N bond lengths of the aminocyclopentadienyl systems are also worth noting. The C−N distance of 1.380 Å for **2** is close to the average of 1.395 Å reported for the previous 18-electron systems.[43,44] There is significant lengthening of the C−N bond (to 1.461 Å) approaching the single-bond C−N distance of 1.47 Å, in contrast to the shortening reported for the same bonds in aminoferrocenium complexes.[44c]

Crystalline [**3**][B(C₆F₅)₄] is an air-sensitive turquoise solid, the structure of which is shown in Figure 7. Table 2 lists the collection parameters and crystal data for this sample, and Table 4 lists important bond distances and angles. The metal is centered 1.768 Å below the C₅Me₅ ring, essentially unchanged from the metal-to-centroid distance of 1.770 Å for neutral **3**, a value calculated using the structural data previously reported[45] for the 18-electron compound. The methyl carbons are out of the plane of the C₅ ring, with the angle of the C−C bond ranging
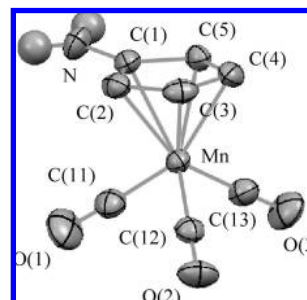


**Figure 6.** Diagram of the molecular structure of **2** with 50% probability ellipsoids. Cp hydrogens omitted for clarity.
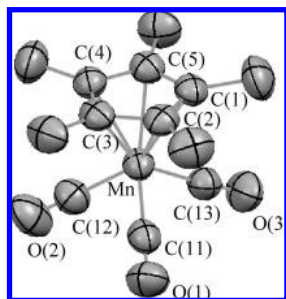
**Figure 7.** Diagram of the molecular structure of [**3**][B(C$_6$F$_5$)$_4$] with 50% probability ellipsoids. Hydrogens and counteranion omitted for clarity.

**Table 4.** Selected Bond Lengths (Å) and Bond Angles (deg) for [Mn($\eta^5$-C$_5$Me$_5$)(CO)$_3$]$^+$, **3**$^+$

| bond | bond length | angle | bond angle |
|---|---|---|---|
| Mn−C(1) | 2.158(4) | C(11)−Mn−C(12) | 87.6(2) |
| Mn−C(2) | 2.137(4) | C(11)−Mn−C(13) | 92.82(19) |
| Mn−C(3) | 2.134(4) | C(12)−Mn−C(13) | 103.76(19) |
| Mn−C(4) | 2.132(4) | O(1)−C(11)−Mn | 178.5(4) |
| Mn−C(5) | 2.150(4) | O(2)−C(12)−Mn | 177.7(5) |
| Mn−C(11) | 1.852(6) | O(3)−C(13)−Mn | 175.3(4) |
| Mn−C(12) | 1.866(5) | | |
| Mn−C(13) | 1.898(4) | | |
| O(1)−C(11) | 1.120(6) | | |
| O(2)−C(12) | 1.119(6) | | |
| O(3)−C(13) | 1.098(5) | | |
| C(1)−C(5) | 1.408(6) | | |
| C(1)−C(2) | 1.416(6) | | |
| C(2)−C(3) | 1.458(6) | | |
| C(3)−C(4) | 1.424(6) | | |
| C(4)−C(5) | 1.403(6) | | |
| Mn-to-center C$_5$ | 1.768 | | |

from 2.0° to 5.6° relative to the ring, bent away from the Mn center. This is not the case for neutral **3**, in which the methyl carbons are apparently in plane with the ring.[45] Another interesting aspect is that one of the C(O)−Mn−C(O) bond angles is severely distorted, increasing to 103.8° from the octahedral value 90°, thereby reducing the symmetry of the cation to $C_s$. A similar distortion computed earlier for the third-row congener [ReCp(CO)$_3$]$^+$ was interpreted as arising from rehybridization of the SOMO, and a similar orbital change may be occurring in the present case. The makeup of the SOMO will be discussed in more detail below. Also of note are the significantly longer Mn−C(O) bonds (average change, $\Delta d$(Mn−C(O)) = + 0.142 Å) and shorter C−O bonds (average change, $\Delta d$(C−O) = −0.063 Å) seen for **3**$^+$ compared to **3**, changes that are qualitatively explained by the weakening of metal-to-carbonyl back-bonding in the radical cation. However, the magnitudes of the changes are surprisingly large, especially in view of the observation of much smaller changes for **2**$^+$ from **2** ($\Delta d$(Mn−C(O)) = + 0.006 Å, $\Delta d$(C−O) = −0.003 Å, average values). Significantly smaller changes have also been computed for the congeneric analogous pair [ReCp(CO)$_3$]$^+$ and ReCp(CO)$_3$.[27b] It is relevant to compare these bond-length changes to those recently described for the Mn(CO)$_3$ moiety in the successive one-electron *reductions* of Mn(Ph-C$_3$B$_7$H$_9$)(CO)$_3$ to [Mn(Ph-C$_3$B$_7$H$_9$)(CO)$_3$]$^n$ ($n = -1, -2$).[46a] When the changes

are written as going from more-to-less-reduced systems in concert with the signs of $\Delta$ used for the presently described oxidations, values of $\Delta d$(Mn−C(O)) = + 0.023 Å and $\Delta d$(C−O) = − 0.011 Å were obtained when going from $n = -2$ to $n = -1$, and $\Delta d$(Mn−C(O)) = +0.013 Å and $\Delta d$(C−O) = −0.008 Å, in going from $n = -1$ to $n = 0$. In the case of the carboranyl system, the smaller bond-length changes might be ascribed to the high degree of electronic delocalization in the reduced species.[46a] The largest redox-induced M−C(O) bond length changes in half-sandwich complexes of which we are aware are those reported by Connelly et al. for the one-electron oxidation of the monocarbonyl complexes WTp′(CO)X($\eta$-C$_2$Me$_2$) (Tp′ = tris(3,5-dimethylpyrazolyl)borate, X = Cl or Br).[46b] In those cases, increases in $d$(W−C(O)) of +0.176 Å and + 0.146 Å were observed for the Br and Cl complexes, respectively, and the C−O distances decreased by −0.084 Å (X = Br) and −0.060 Å (X = Cl). A collection of earlier redox-induced changes in M−C(O) bond lengths is available.[46c]

The fact that the distance from the metal to the center of the C$_5$ ring changes so little for either **2/2**$^+$ or **3/3**$^+$ is surprising, given that significant elongation of the iron-to-ring distance occurs when ferrocene systems are oxidized to ferrocenium ions. For example, compared to their 18-electron counterparts, increases of 0.044 and 0.05 Å have been reported for the ferrocenium[47a,b] and decamethylferrocenium ions.[47c,d]

**ESR.** The three radical cations were all ESR-silent in fluid solution but strongly resonant in frozen solution at 77 K (Figure 8). A spectrum of **1**$^+$ recorded at 4 K was essentially unchanged from that at the higher temperature. As a group, the spectra may be viewed as exhibiting axial or nearly axial behavior, showing hyperfine splittings (hfs, $A$) that are consistent with coupling to a single $^{55}$Mn nucleus ($I = ^5/_2$, 100% abundant). The clearest evidence of deviation from axial behavior was in the perpendicular region of **2**$^+$, wherein there is some complexity in the highest field features of the expected $A_\perp$ hextet. The lower molecular symmetry imparted by substitution at a single cyclopentadienyl position in **2**$^+$ is the likely origin of this spectral deviation, which we believe to be sufficiently modest to allow interpretation of this spectrum as axial, along with those of **1**$^+$ and **3**$^+$. The g- and A-values for this series of radicals are collected in Table 5.

The Mn hfs were used to obtain an estimate of the % Mn character of the SOMO orbitals, using the expressions[48]

$$A_\| = A_{iso} + 2b_o \quad (1)$$

$$A_\perp = A_{iso} - b_o \quad (2)$$

where $A_{iso}$ is the isotropic hfs and $b_o$ is the uniaxial hyperfine parameter.[49a] Calculation of $b_o$ requires that the relative signs of $A_\|$ and $A_\perp$ be either known through additional experimental

(45) (a) Fortier, S.; Baird, M. C.; Preston, K. F.; Morton, J. R.; Ziegler, T.; Jaegar, T. J.; Watkins, W. C.; MacNeil, J. H.; Watson, K. A.; Hensel, K.; Le Page, Y.; Charland, J.; Williams, A. J. *J. Am. Chem. Soc.* **1991**, *113*, 542. (b) For an earlier paper, see: Morton, J. R.; Preston, K. F.; Cooley, N. A.; Baird, M. C.; Krusic, P. J.; McLain, S. J. *J. Chem. Soc., Faraday Trans. 1* **1987**, *83*, 3535.

(46) (a) Nafady, A.; Butterick, R., III; Calhorda, M. J.; Carroll, P. J.; Chong, D.; Geiger, W. E.; Sneddon, L. G. *Organometallics* **2007**, *26*, 4471. (b) Adams, C. J.; Bartlett, I. M.; Carlton, S.; Connelly, N. G.; Harding, D. J.; Hayward, O. D.; Orpen, A. G.; Patron, E.; Ray, C. D.; Rieger, P. H. *J. Chem. Soc., Dalton Trans.* **2007**, 62. (c) Orpen, A. G.; Connelly, N. G. *Organometallics* **1990**, *9*, 1206.

(47) (a) Sullivan, B. W.; Foxman, B. M. *Organometallics* **1983**, *2*, 187. (b) Martinez, R.; Tiripicchio, A. *Acta Crystallogr.* **1990**, *C46*, 202. (c) Freyberg, D. P.; Robbins, J. L.; Raymond, K. N.; Smart, J. C. *J. Am. Chem. Soc.* **1979**, *101*, 892. (d) Pickardt, J.; Schumann, H.; Mohtachemi, R. *Acta Crystallogr.* **1990**, *C46*, 39.

(48) Ayscough, P. B. *Electron Spin Resonance in Chemistry*; Methuen & Co.: London, 1967; pp 82−84.

(49) (a) Weil, J. A.; Bolton, J. R.; Wertz, J. E. *Electron Paramagnetic Resonance*; John Wiley & Sons: New York, 1994; pp 114−116. (b) *Ibid.*, p 534.
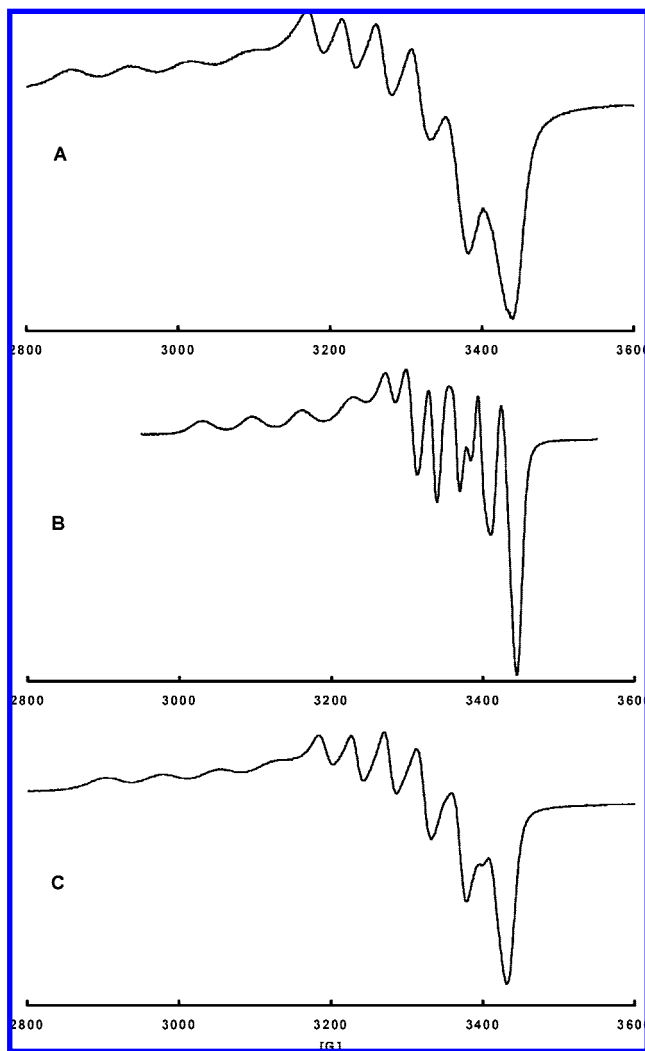
**Figure 8.** ESR spectra of (A) **1**$^+$, (B) **2**$^+$, and (C) **3**$^+$ at 77 K. Samples were prepared by exhaustive electrolysis of the respective neutral species in CH$_2$Cl$_2$/0.05 M [NBu$_4$][B(C$_6$F$_5$)$_4$] at 253 K.

**Table 5.** Summary of ESR Results for [Mn(C$_5$R$_4$R′)(CO)$_3$]$^+$

| radical | $g_\parallel$ | $g_\perp$ | $A_\parallel{}^a$ (G) | $A_\perp{}^b$ (G) | % Mn (d) |
|---------|------|------|------|------|------|
| **1**$^+$ | 2.213 | 2.079 | 79.2 | 50 | 49 |
| **2**$^+$ | 2.120 | 2.011 | 65.1 | 47 | 47 |
| **3**$^+$ | 2.118 | 2.044 | 76.5 | 30 | 36 |

$^a$ Known with certainty. $^b$ Value based on best estimate from outer branches of six-line pattern.

information or assumed on the basis of theory or chemical intuition. The experimental approach, which requires measurement of $A_{iso}$ and takes advantage of the relationship $3A_{iso} = (A_\parallel + 2A_\perp)$, was not possible in the present case owing to the lack of observable fluid spectra. Values of $b_o = 9.7$ and 43.1 G are calculated if the signs of $A_\parallel$ and $A_\perp$ are either the same or different, respectively. Since the theoretical value calculated for the uniaxial parameter when the unpaired electron is located exclusively in a Mn d-orbital is 88 G,[49b] the % Mn character of the SOMO is either 11% for the smaller $b_o$ option or 49% for the larger. Given that the HOMO of **1** is certain to contain significant metal character,[6,16–19] the latter is much more likely and it was therefore assumed that $A_\parallel$ and $A_\perp$ were of different sign for all three radicals. The % Mn d-orbital character is estimated, thusly, to be 49% in **1**$^+$, 36% in **2**$^+$, and 47% in **3**$^+$.

Since the neutral radical CrCp(CO)$_3$ is isoelectronic with **1**$^+$, it is of value to compare the present data with those reported earlier for the chromium complex.[45,50] Based on spectra of a dilute single-crystal of CrCp(CO)$_3$ in MnCp(CO)$_3$, the SOMO was shown to have about a 40% Cr 3d character.[51,52] In terms of Mn analogues of **1**$^+$–**3**$^+$, only spectra of carbonyl-substituted 17-electron Mn complexes have been reported. The most detailed studies have been done on the disubstituted complexes [MnCp(CO)L$_2$]$^+$, L = PMe$_3$ or PPh$_3$, [MnCp(CO)L′]$^+$, L′ = bisphosphino ligand, and the monosubstituted complex [MnCp(CO)$_2$(PPh$_3$)]$^+$.[53] Each of the CO-substituted radicals gave decidedly rhombic ESR spectra and had the complication of showing significant misalignments between the axes of the g-tensor and the $^{55}$Mn A-tensor. Nevertheless, Pike et al. were able to conclude that the SOMOs contained about $^2/_3$ Mn character, the d-orbital being a hybrid of d$_{x^2-y^2}$, d$_{xz}$, and d$_{z^2}$ orbitals created by spin−orbit coupling.[53] Spectra have also been reported for piano-stool Mn radicals in which one carbonyl has been replaced by a single-electron donor. These include MnCp*(CO)$_2$L, L = SR,[54] MnCp(CO)$_2$(RNH),[55] Mn(C$_5$H$_{5-n}$Me$_n$)-(CO)$_2$NR$_2$,[56] [MnCp(CO)$_2$(4-cyanopyridine)]$^-$,[57] and MnCp(CO)$_2$-L′, L′ = RC$_6$H$_4$NH.[57] In those cases, however, the complexes were shown to be essentially organic radicals stabilized by bonding to the MnCp(CO)$_2$ moiety.

Also informative are the g-values of **1**$^+$–**3**$^+$, for those of d$^5$ metal sandwich and half-sandwich systems have undergone considerable analysis.[50,52,58–61] A key factor is the influence of the separation of the ground and excited states on the g-values and relaxation rates of the radicals, a separation which is determined in large part by the splittings of the three frontier orbitals referred to earlier. A smaller energy separation leads to a greater deviation of g from the free-spin value $g_e$ (= 2.0023) and a more rapid electronic relaxation. The latter is the reason why low temperatures (often well below 77 K) are needed for detection of highly symmetric d$^5$ radicals such as the ferrocenium ion.[58] Such systems often have one g-value which is considerably below 2.0. When the near-degeneracy of the largely

(50) Krusic, P. J.; McLain, S,J.; Morton, J. R.; Preston, K. F.; LePage, Y. *J. Magn. Reson.* **1987**, *74*, 72.

(51) This value of 40% Cr spin is based on the correction of the data in ref 50 by Rieger in ref 53.

(52) Rieger, P. H. *Coord. Chem. Rev.* **1994**, *135/136*, 203.

(53) Pike, R. D.; Rieger, A. L.; Rieger, P. H. *J. Chem. Soc., Faraday Trans. 1* **1989**, *85*, 3913.

(54) Winter, A.; Huttner, G.; Zsolnai, L.; Kroneck, P.; Gottlieb, M. *Angew. Chem., Int. Ed.* **1984**, *23*, 975.

(55) (a) Sellmann, D.; Müller, J.; Hofmann, P. *Angew. Chem., Int. Ed.* **1982**, *21*, 691. (b) Sellmann, D.; Müller, J. *J. Organomet. Chem.* **1985**, *281*, 249.

(56) (a) Gross, R.; Kaim, W. *Inorg. Chem.* **1987**, *26*, 3596. (b) Gross, R.; Kaim, W. *J. Chem. Soc., Faraday Trans. 1* **1987**, *83*, 3549.

(57) Gross, R.; Kaim, W. *Angew. Chem., Int. Ed.* **1985**, *24*, 856.

(58) Ammeter, J. H. *J. Magn. Reson.* **1978**, *30*, 299.

(59) (a) Elschenbroich, C.; Bilger, E.; Möckel, R. *Z. Naturforsch. B* **1983**, *38*, 1357. (b) Elschenbroich, C.; Möckel, R.; Bilger, E. *Z. Naturforsch. B* **1984**, *39*, 375.

(60) Elschenbroich, C.; Bilger, E.; Ernst, R. D.; Wilson, D. R.; Kralik, M. S. *Organometallics* **1985**, *4*, 2068.

(61) Hoobler, R. J.; Hutton, M. A.; Dillard, M. M.; Castellani, M. P.; Rheingold, A. L.; Rieger, A. L.; Rieger, P. H.; Richards, T. C.; Geiger, W. E. *Organometallics* **1993**, *12*, 116.

(62) (a) Chong, D.; Geiger, W. E.; Davis, N. A.; Weisbich, A.; Shi, Y.; Arif, A. M.; Ernst, R. D. *Organometallics* **2008**, *27*, 430. (b) LeSuer, R.; Basta, R.; Geiger, W. E.; Arif, A. M.; Ernst, R. D. *Organometallics* **2003**, *22*, 1487.

(63) An exception to this generalization is that fluid spectra may be obtained for high-symmetry radicals having a $^2$A ground state (see ref 59 as well as (a) Elschenbroich, C.; Mockel, R.; Vasil'kov, A.; Metz, B.; Harms, K. *Eur. J. Inorg. Chem.* **1998**, *10*, 1391).
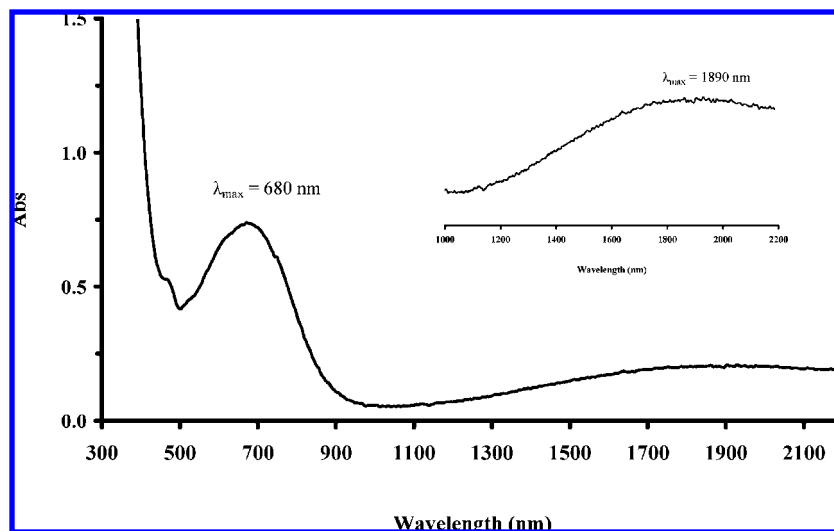
**Figure 9.** UV−vis/near-IR spectrum of 3.3 mM $3^+$ in CDCl$_3$ at 298 K. Sample prepared by chemical oxidation of **3** with [(ReCp(CO)$_3$)$_2$][B(C$_6$F$_5$)$_4$]$_2$ in CDCl$_3$.

metal-based frontier orbitals is lifted significantly through symmetry lowering or orbital mixing, ESR spectra are generally observed at higher temperatures, perhaps even in fluid media, and the lowest $g$-value is found near 2.0.[60,62,63] In the present case, none of the $g$-values were below $g_e$ and the spectra, although well visible at 77 K, were too broad to measure in fluid solution. These facts are qualitatively suggestive that there is only a modest separation of the ground and first excited states of $1^+$−$3^+$, a point that was explored more quantitatively through the near-IR absorptions of the radicals (*vide infra*).

One further point is that the individual lines in the spectra show no anomalous variations in line width. This is in contrast to the findings of Castellani et al. on the spectra of [MnCp-(CO)(dmpe)]$^+$ (dmpe = bis(dimethylphosphino)ethane) cation radical and analogous chromium half-sandwich radicals.[64] In particular, the dramatic narrowing of the low-field "parallel" features of hyperfine lines with increased $|m_I|$ values in [MnCp-(CO)(dmpe)]$^+$ was ascribed to the noncoincidence of the principal axes of the $g$- and $A$-tensors. In the present case, at least three of the parallel lines were well resolved and the breadths of the $m_I = {}^5/_2$, ${}^3/_2$, and ${}^1/_2$ lines were essentially unchanged,[65] having widths at half-height of 30−35 G. The lack of line width anomalies is taken as evidence that the $g$- and $A$-tensors of $1^+$−$3^+$ are not significantly misaligned, increasing the credibility of the simple axial model used here to estimate the degree of Mn character in the SOMO. It should be mentioned, however, that the ESR properties of piano-stool radicals may be quite complex, with the relative ordering of the SOMO and next-highest filled orbital being sensitive even to environmental effects,[64] and that more detailed studies of the Mn(II) tricarbonyl complexes, ideally on diluted single crystals, are warranted.

**Visible and Near-IR Spectroscopy.** All three cation radicals exhibit a strong absorption in the visible region, as well as a weaker absorption in the near-IR, Figure 9 for $3^+$ being typical. From the values of $\lambda_{max}$ and $\epsilon$ given in Table 6 it can be seen

(64) Castellani, M. P.; Connelly, N. G.; Pike, R. D.; Rieger, A. L.; Rieger, P. H. *Organometallics* **1997**, *16*, 4369.

(65) An exception to this generalization is that the four observed "parallel" features of $1^+$ increased in width going from lower-to-higher field in a spectrum recorded at 10 K.

**Table 6.** UV−vis, near-IR, $^1$H NMR Results for $1^+$, $2^+$, and $3^+$ as [B(C$_6$F$_5$)$_4$] Salts

| | $1^+$ | $2^+$ | $3^+$ |
|---|---|---|---|
| $\lambda_{max}$ (cm$^{-1}$) ($\epsilon$, cm$^{-1}$ M$^{-1}$) | 18 850 (1010) | 12 320 (1066) | 14 700 (225) |
| $\lambda_{max}$ (cm$^{-1}$) ($\epsilon$, cm$^{-1}$ M$^{-1}$) | 4840 (64) | 6490 (97) | 5280 (56) |
| $^1$H NMR chemical shift (ppm vs TMS) | 22.4[a] | −23.9, 26.4 | 44.7 |
| $^1$H NMR paramagnetic shift (ppm) (line width, Hz)[b] | 17.7 (234)[a] | −27.0 (1970),[c] 22.0 (1010) | 42.8 (294) |

[a] Prepared by controlled potential coulometry, >90% yield as determined by coulomb count and LSV. Presence of neutral species would result in false low values (see text). [b] Width taken at half-height. [c] Value calculated on the assumption that this peak is due to amine protons.

that the visible band, most likely arising from ligand-to-metal charge transfer, red-shifts significantly in going from $1^+$ ($\lambda_{max}$ = 530 nm) to $3^+$ (680 nm) to $2^+$ (811 nm). More unusual are the weaker absorptions (magnified in the inset of Figure 9 for $3^+$, $\epsilon \approx 50{-}100$ M$^{-1}$ cm$^{-1}$) seen at very low energy in the near-IR region. Absorptions of this type were first reported for the piano-stool radicals Cr($\eta^5$-C$_5$Ph$_5$)(CO)$_3$ and [MnCp(CO)$_2$-(PPh$_3$)]$^+$ [66] and are attributed to metal−metal transitions arising from splitting of the close-lying electronic states of the radical cations. The significant blue shift of the near-IR transition of $2^+$ compared to $1^+$ or $3^+$ is consistent with the earlier hypothesis which predicted shifts to higher energies for piano-stool radicals having lower symmetry.[66]

In order to further probe these low-energy absorptions, we measured the near-IR absorption energies of a wider range of Mn half-sandwich cation radicals, many of which are easily obtained as their [PF$_6$]$^-$ salts by oxidation of the corresponding 18 e$^-$ compounds in which one or more carbonyl groups have been substituted by donor ligands.[9,10,34,35,38] Near-IR bands were measured for 10 compounds in this study, varying in $\lambda_{max}$ from 2066 nm (for $1^+$) to 1470 nm (for [MnCp(CO)(PPh$_3$)$_2$]$^+$), and for all but $2^+$, a reasonably good correlation was observed between an increase in the absorption energy and a decrease in the anodic $E_{1/2}$ potential (see Figure 10). The splitting of the

(66) Atwood, C. G.; Geiger, W. E. *J. Am. Chem. Soc.* **1994**, *116*, 10849.
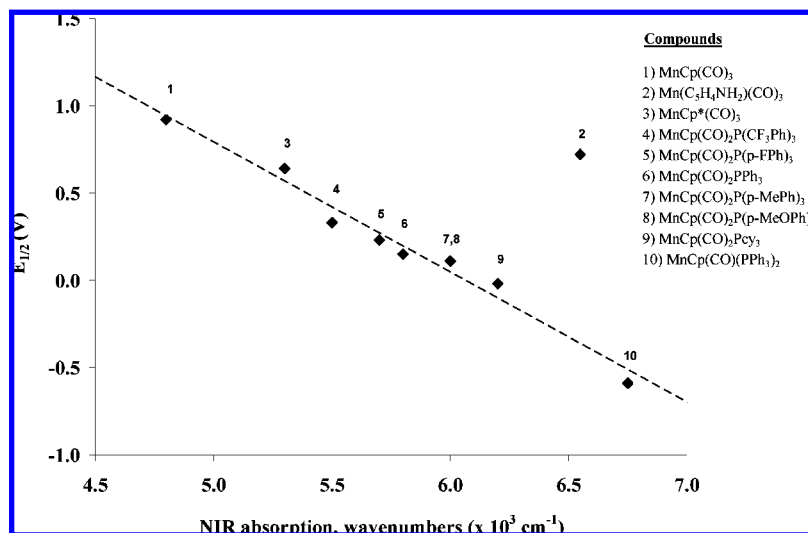
**Figure 10.** Relationship between energy of carbonyl absorption or oxidation potential and energy of near-IR transition for selected Mn piano-stool complexes.
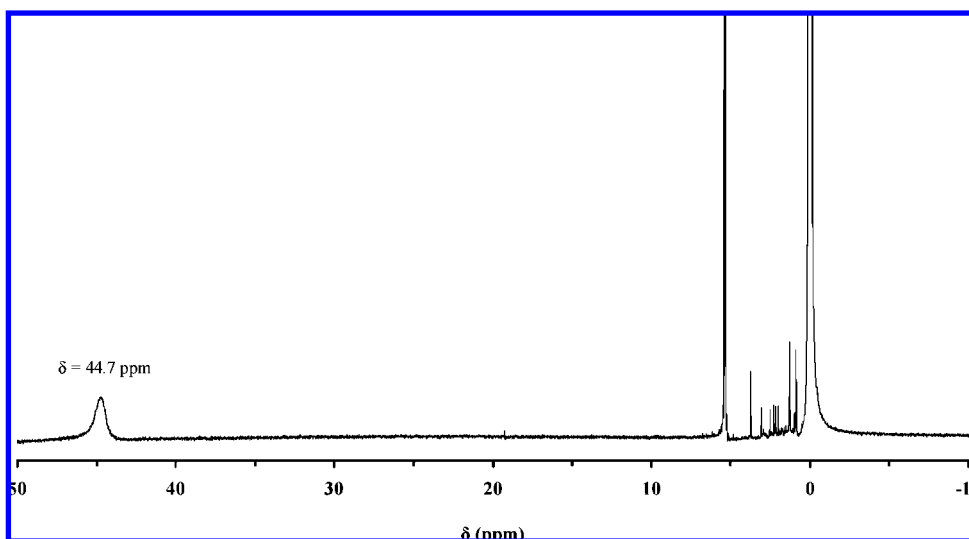


**Figure 11.** $^1H$ NMR spectrum of $3^+$ in $CD_2Cl_2$.

closely lying orbitals, assigned as a′ and a″ in the Mn-phosphine radicals,[38] is thus shown to increase with an increase in phosphine donor strength.

The observed orbital splitting energies have a relationship to the ESR $g$-values. Using a simple metal-localized model for octahedral $d^5$ systems,[67] it can be shown[45] that the difference between $g_z$ and the free-spin value $g_e$ is related to the energy difference, $\Delta$, between the ground and nearest excited state by the relationship $g_z - g_e = 2\lambda_{SO}/\Delta$, where $\lambda_{SO}$ is the spin−orbit coupling constant of the metal. Using $\lambda_{SO} = 300$ cm$^{-1}$ for Mn(II),[67] and assuming that the highest $g$-value is $g_z$,[45] a value of $\Delta = 5170$ cm$^{-1}$ is predicted for the low-energy optical transition for $3^+$, comparing well with the measured energy of 5280 cm$^{-1}$. This excellent agreement for $3^+$ is seen to be fortuitous, however, when the other radicals in this series are similarly treated with the calculated values being generally too low (for $1^+$, 2840 cm$^{-1}$ calculated compared to 4840 cm$^{-1}$ measured; for $2^+$, 5085 cm$^{-1}$ calculated compared to 6490 cm$^{-1}$

measured). It is not surprising to see the lack of quantitative agreement between the $g$-values and the energies of the near-IR bands, given the underlying assumptions, especially in ignoring the ligand contributions to the orbitals involved. Still, this model does account qualitatively for the absorbances observed for this family of radicals in the near-IR to the edge of the midrange IR region.

Finally, inspection of Figure 10 shows that complex $2^+$ is an outlier in the inverse correlation of the near-IR transition energy with the anodic $E_{1/2}$ values. Amino-substitution of the Cp ring apparently has the effect of increasing the splitting of metal orbitals significantly beyond the extent expected on the basis of a simple cyclopentadienyl substituent effect.

**Paramagnetic NMR.** The fast electronic relaxation responsible for the lack of fluid-medium ESR signals suggested that the radicals would show NMR activity.[68,69] Indeed, both $1^+$ and

(67) Goodman, B. A.; Raynor, J. B. *Adv. Inorg. Chem. Radiochem.* **1970**, *13*, 135.

(68) Bertini, I.; Luchinat, C. In *Physical Methods for Chemists*, 2nd ed.; Drago, R. S., Ed.; Saunders College Publishing: Ft. Worth, TX, 1992; pp 519 ff.

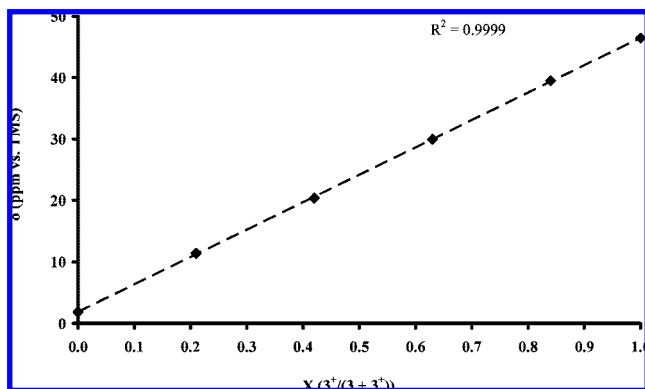(69) Satterlee, J. D. *Concepts Magn. Reson.* **1990**, *2*, 119.

**Figure 12.** Plot of $^1$H NMR paramagnetic shift vs mole fraction of $3^+$ in $CD_2Cl_2$.

$3^+$ displayed a single, strong $^1$H NMR signal shifted to high frequency ($\delta = 22.4$ ppm vs TMS for $1^+$,[70] width at half-height $= 230$ Hz; 44.7 ppm vs TMS for $3^+$, width at half-height $= 295$ Hz, Figure 11). The resonance for the Cp* compound was tracked carefully with the addition of neutral **3** and $3^+$, and the precise linear fit of chemical shift vs fraction of radical (Figure 12) established the integrity of the spectral assignment and the fact that the self-exchange rate of $3/3^+$ is rapid. If the position of the resonance is dominated by contact shifts, its direction is determined by the sign of the $\pi$ spin density in the radical, a positive shift (to higher frequency) being the product of a positive spin density.[71] The fact that the shifts are positive for *both* $1^+$ and $3^+$ is unanticipated, as the contact interactions are expected to have the opposite sign for $1^+$, where the spin on H should be dominated by McConnell-type C–H spin polarization,[72] and $3^+$, where the spin on the methyl hydrogen should be dominated by hyperconjugation.[73] Dipolar effects (*pseudo*-contact interactions) may prove to be responsible for the unidirectional chemical shifts for $1^+$ and $3^+$, but more in-depth treatments will be necessary to delineate the influence of contact *vs pseudo*-contact interactions in these radicals. As observed earlier with ferrocenium-type species, interpretation of the chemical shifts of paramagnetic metallocenes is not straightforward,[74] and Cp-derivatization[75] may be necessary to sort out the dominant shift mechanisms in the Mn system.

A spectrum was also observed for $2^+$, broad peaks being seen at 26.4 ppm (width at half-height $= 1010$ Hz) and $-23.9$ ppm (width at half-height $= 1970$ Hz) vs TMS. The fact that these peaks integrated to a 1:1, rather than the expected 2:1, ratio obscures their assignments, but the low field signal at $-23.9$ ppm may be tentatively assigned to the amino hydrogens based on comparison with the shift reported for the amino-ferrocenium analogue $[Fe(C_5H_4NH_2)_2]^+$.[76]

**Nature of the SOMO of $1^+$.** The three highest filled orbitals of $MnCp(CO)_3$ are best described as originating from a $t_{2g}$-like

triad set of the $d^6$ $[Mn(CO)_3]^+$ fragment which mixes weakly with the $Cp^-$ orbitals to form the HOMO to HOMO-2 of this system.[16] Small energy separations of these orbitals occur owing to the $C_s$ symmetry of **1**. Idealized drawings of the three d-orbital contributions to these frontier orbitals are shown below, labeled according to $C_s$ symmetry. The $1a'$ and $1a''$ orbitals, which are derived from the erstwhile $e_g$ pair, are primarily $d_{x^2-y^2}$ mixed with $d_{yz}$ (for $1a'$) and $d_{xy}$ mixed with $d_{xz}$ (for $1a''$) and contain less Cp character than the more metal-based $2a'$ ($d_{z^2}$) orbital. It is important to keep in mind that these orbitals also have significant carbonyl character. The earlier, quite detailed, ESR studies on piano-stool radicals are in agreement that the SOMO may be either $1a'$ or $1a''$, the ordering being sensitive to ligand changes. For the two systems closest to the present radicals, namely $CrCp(CO)_3$[45,50] and $[MnCp(CO)_2(PPh_3)]^+$,[53] a $1a''$ SOMO was favored. Although our data on the Mn systems $1^+$ and $3^+$ are certainly consistent with those findings, the assignment of their SOMOs as $1a''$ must be tempered by the fact that delineation between the two possibilities of $1a'$ and $1a''$ is difficult.[45] However, it seems safe to conclude that the SOMOs of $1^+$ and $3^+$ have *ca.* 50% of a hybrid Mn d-orbital, most of the remaining spin presumably being in the carbonyl groups. The degree of metal character in the SOMO has now been shown to be in a range of about 36–67% for a number of $d^5$ piano-stool compounds.[45b,50,51,53]
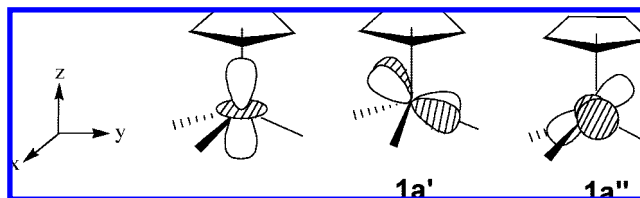


The ESR results on $2^+$ differ only quantitatively from those of $1^+$ and $3^+$, with slightly smaller Mn hyperfine splittings. However, as pointed out previously, the near-IR absorption stands out as falling at considerably higher energy than observed for the other members of this family. This is most likely to arise from an unexpectedly large splitting of the $^2A''$ and $^2A'$ states, but a change in the nature of the SOMO of $2^+$ cannot be ruled out. To this point, we note that both the calculated % Mn character of the SOMO and the weighted average carbonyl-IR shifts are smaller for $2^+$ than for $1^+$, suggesting the presence of a significant amount of spin and charge at the $NH_2$ group of the former.

## Conclusions

The cymantrene radical cation $1^+$ can be electrochemically generated and spectrally monitored at room temperature in a low-donor solvent containing a weakly coordinating electrolyte anion. It has a rich, and perhaps unprecedented, breadth of spectral responses in that it is active in the visible, near-IR, and IR ($\nu_{CO}$) ranges and exhibits both NMR and ESR activities, the latter showing Mn hyperfine splittings. The near-IR absorption and the magnetic resonance responses are all consistent with an electronic model of $1^+$ in which an excited state lies fairly close in energy to the ground state, accounting for its absorption band at 4840 cm$^{-1}$ and the rapid electronic relaxation that makes it ESR-inactive and NMR-active at room temperature. The SOMO of $1^+$ contains about 50% Mn d-orbital character, with a significant contribution also from the carbonyl groups and, presumably, a smaller contribution from the Cp ligand. The fact that considerable ligand character is found in

(70) Owing to the difficulty of maintaining a pure sample of $1^+$ in solution at room temperature under NMR conditions, a small amount of **1** was apparently present in this sample.
(71) Satterlee, J. D. *Concepts Magn. Reson.* **1990**, *2*, 69.
(72) McConnell, H. M. *J. Chem. Phys.* **1963**, *39*, 1910.
(73) Carrington, A.; McLachlan, A. D. *Introduction to Magnetic Resonance*; Harper & Row: New York, 1967; pp 83–85, 109–110.
(74) Blümel, J.; Hebendanz, N.; Hudeczek, P.; Köhler, F. H.; Strauss, W. *J. Am. Chem. Soc.* **1992**, *114*, 4223.
(75) Gattinger, I.; Herker, M. A.; Hiller, W.; Köhler, F. H. *Inorg. Chem.* **1999**, *38*, 2359.
(76) Shafir, A.; Power, M. P.; Whitener, G. D.; Arnold, J. *Organometallics* **2000**, *19*, 3978.

the SOMO is consistent with earlier He(I) and He(II) PES results on **1** and its derivatives.[6]

Functionalization of the cyclopentadienyl ring affected the $E_{1/2}$ potential of the 18 $e^-$/17 $e^-$ couple in predictable ways and enhanced both the thermodynamic and kinetic stabilities of the corresponding radical cations. The $E_{1/2}$ values of the aminocyclopentadienyl and Cp* analogues were shifted negative by *ca.* 300 mV, and the radical cations of these systems, **2**[+] and **3**[+], respectively, were isolated and structurally characterized. The distance from the metal to the center of the $C_5Me_5$ ring was essentially unchanged in **3**[+] compared to its 18-electron counterpart, in contrast with the lengthening of 0.05 Å observed in going from decamethylferrocene to the corresponding ferrocenium ion, suggesting that the HOMO of **3** (and by inference, that of **1**) has relatively little metal-Cp mixing. There is a meaningful set of structural changes in the two redox states of the aminocyclopentadienyl Mn system, however, with a significant shortening of the Mn—C(N) bond leading to a nearly planar cyclopentadienyl ring in the 17-electron cation. The bond lengths and angles of the $Mn(CO)_3$ moiety are also more highly affected in the oxidation of **2** than in that of **3**.

The spectral activities of the Cp-functionalized radical cations were consistent with those of **1**[+], validating the idea that cymantrenyl redox tags could be monitored using a number of spectroscopic methods. The fact that the radical cations have spectral responses in two regions having few spectral interferences, namely the near-IR and metal—carbonyl IR regions, raises attractive analytical possibilities for a cymantrenyl group as an anodic redox tag. The widespread application of this tag is likely to be limited by its rather positive potential ($E_{1/2}$ = 0.92 V vs ferrocene) and the susceptibility of its radical cation to nucleophilic attack. However, these difficulties may be mitigated by pre- or postlabeling substitution of one or more carbonyl groups by a donor ligand. Negative $E_{1/2}$ shifts of 600 mV or more are possible when a single CO is replaced by a phosphine, phosphite, or other donor ligand.[77,78] As shown in the present paper and in previous publications,[33–37] the CO-substituted compounds largely retain the optical, near-IR, and IR activities of the parent radical. Although the carbonyl-substitution of $MnCp^\gamma(CO)_3$ ($Cp^\gamma$ = generic cyclopentadienyl ligand) is usually carried out photolytically,[28] an electrochemical substitution

process has also been described.[8,79] Given the enhanced stability of cymantrene-type radical cations under the conditions described in the present paper, a simple electrochemically switched substitution process such as that reported[25] for $Cr(\eta^6\text{-benzene})(CO)_3$ should also be possible for cymantrenyl systems, making it possible, in principle, to perform efficient CO substitution processes on a $Mn(C_5H_4)(CO)_3$ moiety attached to a target molecule. Since double substitution of carbonyl groups by small cone-angle donors is possible, postlabeling substitution processes could lower the cymantrenyl potential by 1000 mV or more, and efforts are underway to probe this approach.[80]

Finally, it is instructive to note the difference in behavior of the congener radical cations **1**[+] and $[ReCp(CO)_3]^+$. The latter dimerizes, forming an unsupported Re—Re bond,[27] whereas no evidence for dimerization has been found for the Mn system. This difference is most likely due to the larger size of the Re atom as well as the significant rehybridization undergone by the HOMO when an electron is removed from $ReCp(CO)_3$.[27] In this sense the monomer/dimer tendencies of $[MCp(CO)_3]^+$, M = Mn, Re, are reminiscent of the first-row vs second- and third-row behavior of the neutral 17-electron analogues $MCp(CO)_3$, M = Cr, Mo, W, which show a much greater tendency toward dimerization with the heavier metals.[81]

**Supporting Information Available:** Three voltammograms of **1** and **3** after bulk electrolysis and ^{1}H NMR spectrum of **1**[+] after bulk oxidation of **1** in CDCl$_3$/[NBu$_4$][TFAB]. This material is available free of charge via the Internet at http://pubs.acs.org

JA801930Q

(77) Lever, A. B. P. *Inorg. Chem.* **1990**, *29*, 1271. predicts shifts of −0.60 and −0.57 V for substitution of CO by PPh$_3$ and P(OMe)$_3$, respectively, based on literature data for the oxidation of Cr(CO)$_5$L, L = CO or donor ligand.

(78) The average potential shifts reported for substitution of CO in half-sandwich complexes are −0.65 V for PPh$_3$ and −0.48 V for P(OR)$_3$ (R = Me or Et). See refs 9, 11, 12, 25, 34, and 35 as well as:(a) Yeung, L. K.; Kim, J. E.; Chung, Y. K.; Rieger, P. H.; Sweigart, D. A. *Organometallics* **1996**, *15*, 3891. (b) Pierce, D. T.; Geiger, W. E. *Inorg. Chem.* **1994**, *33*, 373. (c) Connelly, N. G.; Demidowicz, Z.; Kelly, R. L. *J. Chem. Soc., Dalton Trans.* **1975**, 2335.

(79) Note also that, in refs 10 and 11, substitution processes for replacement of a CO group in Mn(C$_5$H$_4$Me)(CO)$_3$ were carried out first by photolytic substitution of CO by a strong donor such as pyridine, followed by electrocatalytic substitution of pyridine by a slightly weaker donor ligand such as phosphine.

(80) Laws, D. R. University of Vermont, unpublished data. The electrochemically substituted complex MnCp(CO)(P(OMe)$_3$)$_2$ has an $E_{1/2}$ value of −0.25 V *vs* ferrocene.

(81) For early references to the group VI analogues, see: (a) Adams, R. D.; Collins, D. E.; Cotton, F. A. *J. Am. Chem. Soc.* **1974**, *96*, 749. (b) Hackett, P.; O'Neill, P. S.; Manning, A. R. *J. Chem. Soc., Dalton Trans.* **1974**, 1625. (c) Wrighton, M. S.; Ginley, D. S. *J. Am. Chem. Soc.* **1975**, *97*, 4246. A list of 26 references on this topic may be found in ref 41a.